

RESEARCH ARTICLE

Open Access



NF90 interacts with components of RISC and modulates association of Ago2 with mRNA

Giuseppa Grasso[†], Charbel Akkawi[†], Celine Franckhauser, Rima Nait-Saidi, Maxime Bello, Jérôme Barbier and Rosemary Kiernan^{*✉}

Abstract

Background: Nuclear factor 90 (NF90) is a double-stranded RNA-binding protein involved in a multitude of different cellular mechanisms such as transcription, translation, viral infection, and mRNA stability. Recent data suggest that NF90 might influence the abundance of target mRNAs in the cytoplasm through miRNA- and Argonaute 2 (Ago2)-dependent activity.

Results: Here, we identified the interactome of NF90 in the cytoplasm, which revealed several components of the RNA-induced silencing complex (RISC) and associated factors. Co-immunoprecipitation analysis confirmed the interaction of NF90 with the RISC-associated RNA helicase, Moloney leukemia virus 10 (MOV10), and other proteins involved in RISC-mediated silencing, including Ago2. Furthermore, NF90 association with MOV10 and Ago2 was found to be RNA-dependent. Glycerol gradient sedimentation of NF90 immune complexes indicates that these proteins occur in the same protein complex. At target RNAs predicted to bind both NF90 and MOV10 in their 3' UTRs, NF90 association was increased upon loss of MOV10 and vice versa. Interestingly, loss of NF90 led to an increase in association of Ago2 as well as a decrease in the abundance of the target mRNA. Similarly, during hypoxia, the binding of Ago2 to vascular endothelial growth factor (VEGF) mRNA increased after loss of NF90, while the level of VEGF mRNA decreased.

Conclusions: These findings reveal that, in the cytoplasm, NF90 can associate with components of RISC such as Ago2 and MOV10. In addition, the data indicate that NF90 and MOV10 may compete for the binding of common target mRNAs, suggesting a role for NF90 in the regulation of RISC-mediated silencing by stabilizing target mRNAs, such as VEGF, during cancer-induced hypoxia.

Keywords: NF90, RISC, mRNA stability, Ago2, RIP

Background

Nuclear factor 90 (NF90) is a double-stranded RNA-binding protein (RBP) that is involved in a plethora of different cellular processes and pathways, such as transcription, splicing, translation, and mRNA stability or degradation [1]. More recently, NF90 was also

linked to microRNA (miRNA) biogenesis and circular RNA (circRNA) stability [2, 3]. NF90 is a ubiquitous and generally abundant protein that has been shown to shuttle from the nucleus to the cytoplasm depending on its phosphorylation status and as a result of several stimuli, such as viral infection or hypoxia [4–6]. During viral infection, cytoplasmic NF90 can bind viral RNAs to enhance or inhibit viral replication, depending on the type of virus [7]. Besides viral RNAs, NF90 can associate with cellular mRNAs to increase their stability or influence their translation [8, 9]. For instance, NF90 was recently shown to play a role in mitosis by

[†]Giuseppa Grasso and Charbel Akkawi contributed equally to this work.

*Correspondence: Rosemary.Kiernan@igh.cnrs.fr

UMR9002 CNRS-UM, Institut de Génétique Humaine-Université de Montpellier, Gene Regulation lab, 34396 Montpellier, France



competing with Staufen-mediated mRNA decay (SMD) for the binding of mitotic mRNAs [10]. NF90 contains two tandem double-stranded RNA-binding motifs (dsRBMs) that were shown to contribute to the binding of the same RNA molecule simultaneously [11, 12]. It was shown that NF90 is able to recognize specific RNA structures, such as minihelix, and that this structure is sufficient for NF90 binding [13, 14]. A sequence motif has also been shown to positively influence NF90 binding to short mRNAs [11]. Therefore, the precise RNA binding mode of NF90 is still not clear and may depend on the type of RNA. Nevertheless, NF90 RNA binding activity is strongly influenced by the heterodimerization with its protein partner nuclear factor 45 (NF45) which leads to thermodynamic stabilization of the complex and enhanced affinity for RNA substrate [15].

Recent findings implicate NF90 in mRNA stability and translation through miRNAs [16], which could suggest an involvement in RISC-mediated gene silencing. RISC-mediated gene silencing is a well-known post-transcriptional gene regulation mechanism that, in humans, was shown to promote translational inhibition and degradation of target mRNAs mainly by recruiting Ago2 protein [17]. Ago2, guided by the sequence complementarity of a miRNA, is able to diffuse along the 3' UTR of target mRNAs recognizing miRNA recognition elements (MRE) and recruiting effector proteins, such as deadenylases and 5'-to-3' exonucleases, in order to inhibit translation and/or trigger mRNA degradation [18]. Interestingly, characterization of the Ago2 interactome identified NF90/NF45 heterodimer as an interactant of Ago2 in the cytoplasm [19], which could suggest a role for NF90/NF45 in RISC-mediated activities.

For Ago2 lateral diffusion to be efficient, it needs the activity of a helicase to disrupt occlusive secondary RNA structures that could interfere with its binding. Moloney leukemia virus 10 (MOV10) is an ATP-dependent helicase that belongs to the Up frameshift (UPF)-like helicase superfamily 1 (SF1). MOV10 binds ssRNA and translocates 5'-to-3' along the target RNA [20]. It was initially shown to inhibit human immunodeficiency virus type 1 (HIV-1) and hepatitis C virus replication as well as LINE-1 retrotransposition [21, 22]. In addition, MOV10 was found to co-localize in P-bodies together with Ago2 and other factors involved in RISC, identifying a role for MOV10 in miRNA-mediated regulation [23]. MOV10 binds in close proximity to UPF1 binding sites to resolve structures and displace RBPs from the 3' UTR of the target mRNA, thereby exposing the MRE for Ago2 binding [20].

Within a mRNA target, MOV10 frequently binds to the 3' UTR, specifically at regions with low conservation and upstream of local secondary structures, consistent with

its 5'-to-3' directional unwinding activity [20]. Moreover, for efficient loading and unwinding, MOV10, like many RNA helicases, needs a single-stranded region of RNA adjacent to a duplex [24]. Consistent with its role in RISC-mediated silencing, MOV10 can regulate the abundance of the mRNAs to which it binds. In particular, it was shown that depletion of MOV10 inhibits translational suppression leading to global stabilization of its target mRNAs [20]. However, in contrast with this observation, MOV10 was also found to increase the expression of a limited subset of mRNAs, in the presence of fragile X mental retardation protein 1 (FMRP1), by inhibiting Ago2 binding. Therefore, the concomitant binding of MOV10 and FMRP on the same mRNA can inhibit the canonical role of MOV10 in RISC [25, 26].

Here, we show that cytoplasmic NF90 interacts with proteins involved in translational repression, RNA stability, degradation, and viral replication. We determined that NF90 interacts with MOV10 as well as Ago2 in an RNA-dependent fashion. Using RNA immunoprecipitation (RIP) analysis, we showed that both proteins can bind the same target mRNAs, as suggested by published CLIP data of MOV10 and NF90. RIP analysis showed that, upon loss of MOV10, association of NF90 with the mRNA targets increased. Similarly, after loss of NF90/NF45, we detected an increase in the association of MOV10 to the selected target mRNAs. To determine whether NF90 binding might impact association of RISC with the mRNA targets, we performed RIP analysis for Ago2. Following loss of NF90, association of Ago2 with target mRNAs increased, which is consistent with the observed decrease in the abundance of the mRNAs. Hypoxia leads to stabilization of specific NF90-associated mRNAs, such as vascular epithelial growth factor (VEGF) mRNA. Interestingly, during hypoxia, the abundance of VEGF mRNA decreased after loss of NF90/NF45, while its association with Ago2 significantly increased. These data suggest that NF90 may be involved in RISC-mediated gene silencing by regulating MOV10 and Ago2 association with target mRNAs. Moreover, our results suggest that this novel role of NF90 might be implicated in the response to cancer-induced hypoxia.

Results

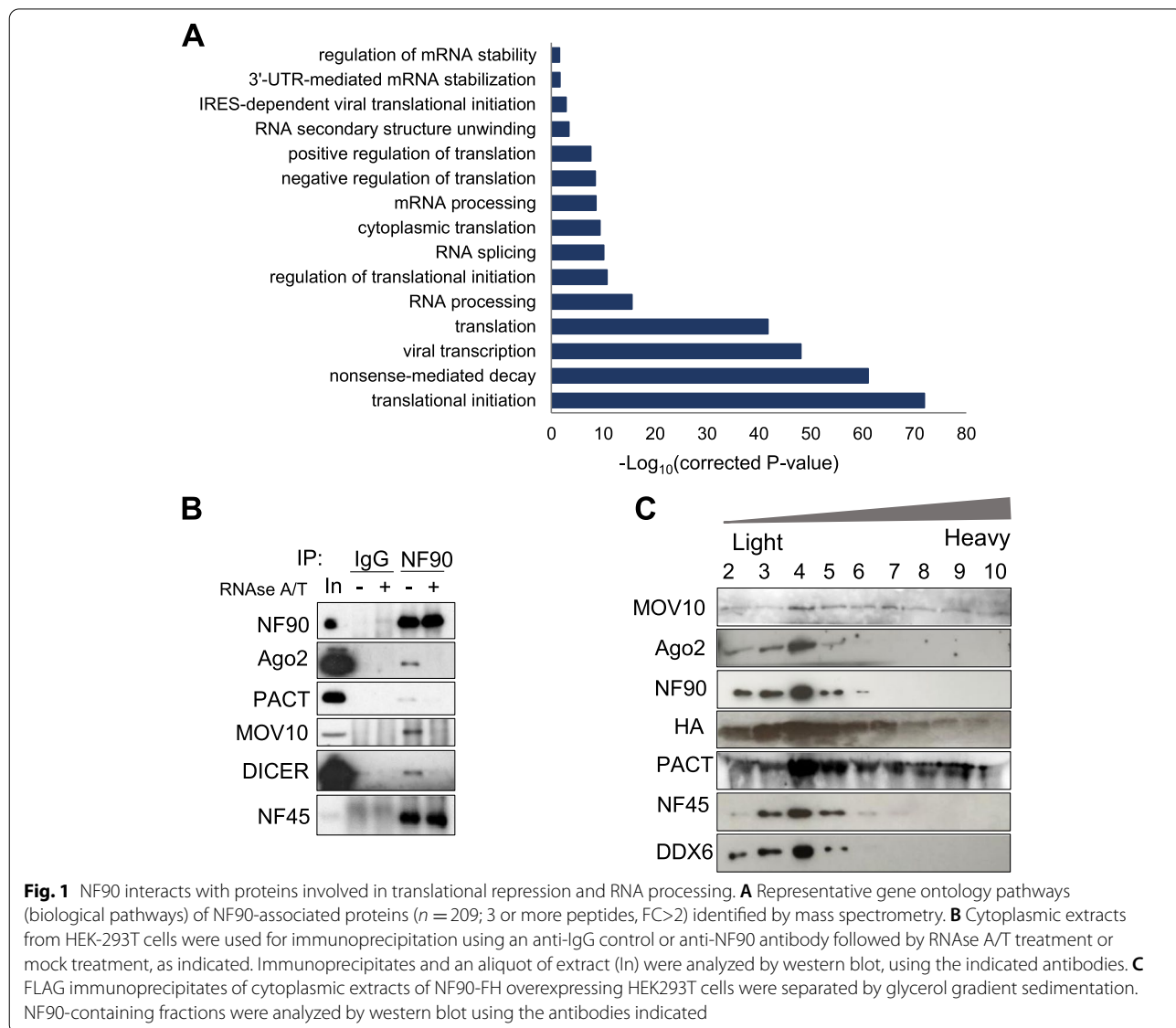
NF90 interacts with proteins involved in translational repression and RNA processing

In order to understand the role of NF90 in the cytoplasm, we determined its cytoplasmic interactome by performing mass spectrometry on a HEK293T cell line stably overexpressing NF90-FLAG-HA (Additional file 1: Fig. S1A), after tandem affinity purification of the cytoplasmic protein fraction (Additional file 1: Fig. S1B). Excluding the proteins for which one peptide or

more was found in the mock HEK293T sample, 318 proteins were detected associated with NF90 in the cytoplasm (Additional file 8: Table S4). Of these, 209 were detected with 3 or more peptides and FC>2 compared to the mock sample (Additional file 8: Table S4). As expected, the most abundant protein identified was NF90 (ILF3). ILF2 (NF45), a well-known NF90 protein partner, was found among the most abundant interactants. Interestingly, several proteins associated with RISC were identified among the interactants. Notably, the 5'-to-3' helicase MOV10 was highly represented. Gene ontology of the significantly enriched NF90 interactants (3 or more peptides, FC>2) identified a number of pathways, such as translation, translational initiation, mRNA processing, and regulation of mRNA stability (Fig. 1A).

These findings are consistent with previous observations suggesting the implication of NF90 in the regulation of mRNA stability and mRNA translation for specific target mRNAs [6, 16].

Since NF90 interactants are well-known RNA-binding proteins (Additional file 1: Fig. S1C), we wondered if their interaction with NF90 was RNA-dependent. In order to validate the results of mass spectrometry using endogenous proteins and to determine if the binding of NF90 is RNA dependent, we performed co-IP in HEK293T cell line, with and without RNase A/T treatment. The binding of NF90 to NF45 was found to be RNA-independent (Fig. 1B), as previously reported [27, 28]. The results confirmed the binding of endogenous NF90 to PACT, MOV10, and Dicer and



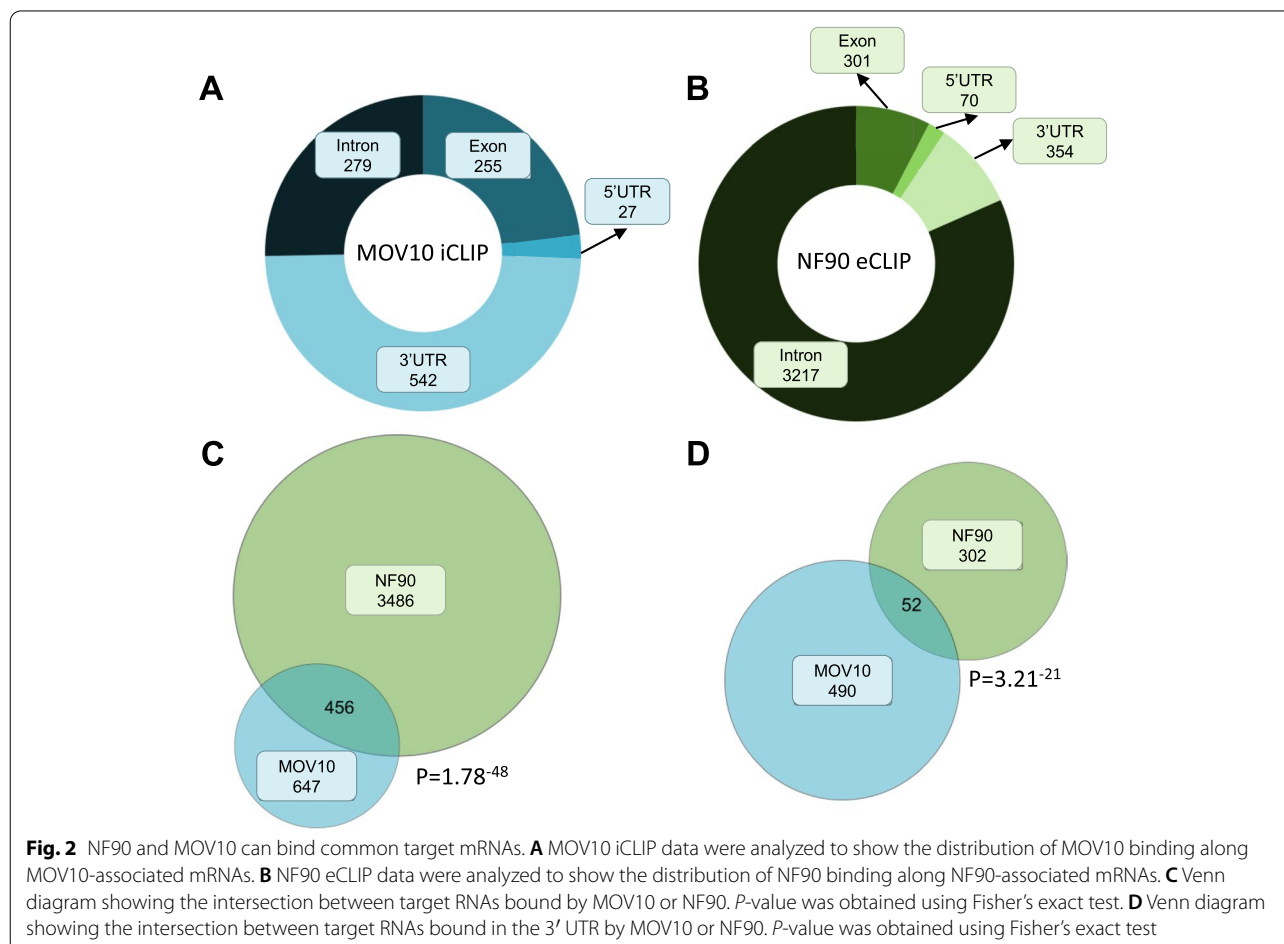
furthermore showed that these interactions are RNA-dependent (Fig. 1B). Since Ago2, the main component of RISC, was also found among NF90 interactants, albeit below the threshold for interactants, we tested its interaction with NF90. Figure 1B shows that Ago2 was associated with NF90, as described previously [19]. Although previously reported to be RNA-independent [19], under the conditions used in this study, NF90 binding to Ago2 was RNA-dependent, in agreement with a recent study [16]. These findings identify an RNA-mediated interaction between NF90 and RISC-silencing complex in the cytoplasm.

To determine whether RISC subunits can be found in the same complex with NF90, we performed glycerol gradient sedimentation of immunopurified NF90-Flag-HA complexes (Additional file 1: Fig. S1D and E). NF90 was detected in the top 10 fractions (data not shown) where it co-sedimented with MOV10, AGO2, PACT, DDX6, and NF45 (Fig. 1C). In agreement with these results, NF90 has been shown to co-sediment with Ago2, NF45 and other helicases, such as DDX47, DDX36, and DDX30, on a sucrose gradient [19]. These

findings suggest that cytoplasmic NF90/NF45 co-sediments with subunits of RISC.

NF90 and MOV10 can bind the same target mRNAs

Among the most abundant interactants of NF90 was MOV10 helicase that is required for optimal RISC activity. To further investigate the interaction between NF90 and MOV10 and a possible role in RISC function, we took advantage of an enhanced UV crosslinking followed by immunoprecipitation of NF90 (eCLIP) [29] and an individual-nucleotide resolution UV crosslinking and IP of MOV10 (iCLIP) [26] datasets. Analysis of MOV10 iCLIP identified 1103 mRNAs significantly bound by MOV10. Approximately half of the bound mRNAs (542 mRNAs) contained a MOV10 peak in the 3'UTR (Fig. 2A), consistent with previous findings suggesting that MOV10 mainly binds 3'UTRs of mRNAs [20]. The remaining MOV10-bound mRNAs contained peaks in introns (279 mRNAs), exons (255 mRNAs) and 5' UTRs (27 mRNAs) (Fig. 2A). On the other hand, analyses of NF90 eCLIP suggest that the majority of mRNAs significantly associated with NF90 were bound in their introns



(3217 out of 3942 NF90-bound mRNAs). However, some mRNAs were also bound in their in exons, 5' UTRs and 3' UTRs (301, 70, and 354, respectively) (Fig. 2B).

Since the interaction between NF90 and MOV10 was found to be RNA-dependent (Fig. 1B), we wondered if these two proteins could bind the same mRNAs. Intersection of the mRNAs bearing at least one peak of NF90 and MOV10 identified 456 mRNAs that could be potentially bound by both proteins (Fig. 2C). Interestingly, this corresponds to around 41% of all mRNAs bound by MOV10 and it is significantly enriched ($P = 1.7e-48$, Fisher's exact test). Next, since the unwinding of 3' UTRs by MOV10 is implicated in RISC-mediated silencing, we wondered whether NF90 and MOV10 were associated with the 3' UTRs of common mRNAs. We identified 52 mRNAs that bear at least one peak of both NF90 and MOV10 in their 3' UTRs (Fig. 2D), which is significantly enriched ($P = 3.21e-21$, Fisher's exact test). These findings suggest that NF90 and MOV10 can bind the 3' UTR of a common set of target mRNAs.

NF90 and MOV10 influence each other's binding to target mRNAs

MOV10 has been shown to facilitate RISC-mediated silencing [23] while, on the contrary, NF90 was found to increase specific target mRNAs stability [9]. We therefore wondered if NF90 could interfere with the binding of MOV10 to the target mRNAs and vice versa. In order to understand the function of NF90 and MOV10 binding to the same target mRNAs, we performed RIP in HEK293T cell line after RNAi against NF90 and NF45 (NF90/NF45), MOV10 or a non-targeting control (Scr), followed by quantitative PCR (qPCR) of target mRNAs selected on the basis of MOV10 iCLIP and NF90 eCLIP analyses (Fig. 2D and Additional file 2: Fig. S2).

RIP of NF90, MOV10, or IgG control was performed after downregulation of MOV10 (Additional file 3: Fig. S3A). Loss of MOV10 did not significantly affect the abundance of the target mRNAs (Additional file 3: Fig. S3B). RIP results revealed that MOV10 association with the selected target mRNAs was significantly decreased after downregulation of MOV10, as expected (Fig. 3). On the other hand, NF90 binding to the same target mRNAs was significantly increased after downregulation of MOV10, while its binding to the negative control, H2BC1, did not significantly change (Fig. 3). Similar results were obtained using a second small-interfering RNA (siRNA) targeting MOV10 (Additional file 4: Fig. S4A and B).

In order to further investigate this mechanism, we performed RIP of NF90, MOV10, or IgG control after downregulation of NF90 and its protein partner NF45 (Additional file 5: Fig. S5A). Interestingly, the loss of

NF90/NF45 significantly decreased the total level of the selected target mRNAs (Additional file 5: Fig. S5B), consistent with its role in increasing mRNA stability [9]. As expected, NF90 association with the target mRNAs was significantly decreased after NF90/NF45 downregulation (Fig. 4). On the other hand, RIP analysis revealed that NF90/NF45 downregulation led to a significant increase in MOV10 association with the selected target mRNAs while its binding to the negative control, H2BC1, did not significantly change (Fig. 4). Similar results were obtained using additional siRNAs targeting NF90 and NF45 (Additional file 6: Fig. S6A and B). These results suggest that the binding of NF90 and MOV10 at common target mRNAs is mutually influenced by the presence of the other factor.

Downregulation of NF90/NF45 complex increases Ago2 binding to target mRNAs

MOV10 is known to promote Ago2 association to mRNAs, thereby enhancing RISC-mediated silencing. Since NF90 and MOV10 influence each other's binding to common target mRNAs, we wondered if alteration of the association NF90/NF45 complex could have similar effects on Ago2 binding to target mRNAs. To this end, we performed RIP of Ago2 or IgG control after downregulation of NF90/NF45. Depletion of NF90/NF45 had no effect on Ago2 expression in extracts or immunoprecipitates (Additional file 7: Fig. S7A and B). Notably, loss of NF90/NF45 significantly increased Ago2 binding to the target mRNAs tested, while the negative control mRNA, H2BC1, which was poorly associated with Ago2, was not significantly increased relative to the IgG control (Fig. 5). Interestingly, the increase in Ago2 binding to target mRNAs is consistent with the observed reduction in the abundance of the same mRNAs following loss of NF90/NF45 (Additional file 5: Fig. S5B).

NF90/NF45 impedes binding of Ago2 to VEGF mRNA during hypoxia

NF90 is known to stabilize VEGF mRNA during cancer-induced hypoxia [6]. We wondered whether the stabilization of VEGF by NF90 during hypoxia might be mediated by the ability of NF90 to influence Ago2 binding to VEGF mRNA. To this end, we performed RIP of Ago2 or IgG control after downregulation of NF90/NF45 and treatment with the hypoxia-inducing drug, CoCl_2 . HEK293T treated with 500 μM of CoCl_2 show increased HIF1 α expression (Fig. 6A), confirming induction of hypoxia, and this concentration was used for further experiments. Depletion of NF90/NF45 had no effect on Ago2 expression in extracts or immunoprecipitates (Fig. 6B, C). However, loss of

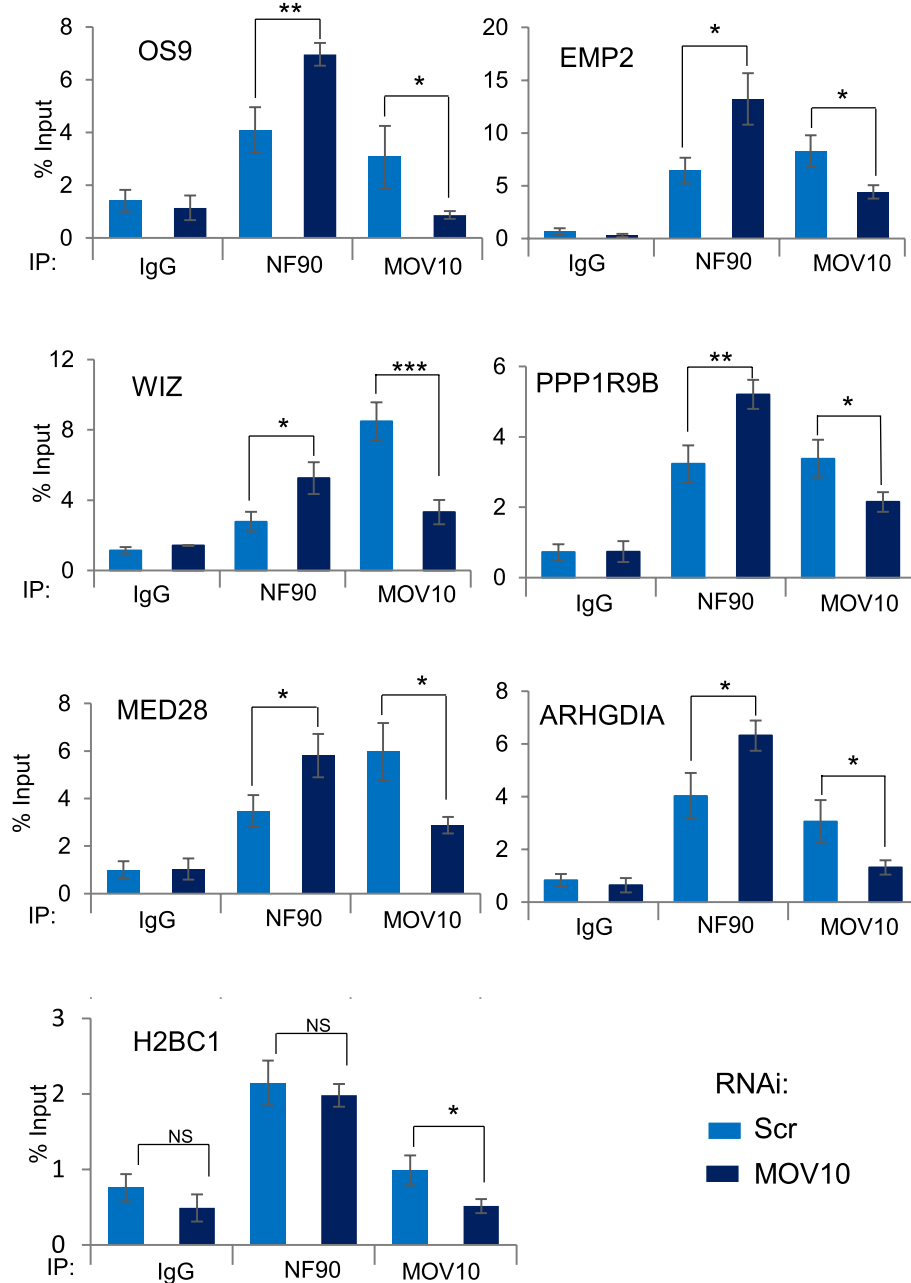


Fig. 3 MOV10 modulates NF90 association with common target mRNAs. RIP analysis of HEK293T cells transfected with MOV10-targeting siRNA or a non-targeting control (Scr), as indicated. RIPs were performed using anti-NF90, anti-MOV10 or a control IgG antibody, as indicated. An aliquot of input and immunoprecipitates were analyzed by RT-qPCR using specific primers, as indicated. Data represent mean \pm SEM obtained from 4 independent experiments (* $P < 0.05$, ** $P < 0.01$, *** $P < 0.001$, NS indicates not significant, independent Student's t test) (Additional file 9)

NF90 significantly decreased the mRNA level of VEGF while increasing the level of H2BC1 mRNA (Fig. 6D). RIP analysis showed that the binding of Ago2 to VEGF mRNA was significantly increased upon loss of NF90/NF45, while the binding to the negative control mRNA, H2BC1, did not significantly change (Fig. 6E).

Discussion

The dsRNA binding protein, NF90, has been implicated in a number of cellular pathways, including the regulation of translation and RNA stability. However, the precise mechanisms involved in its different functions are not entirely clear. To better understand how NF90

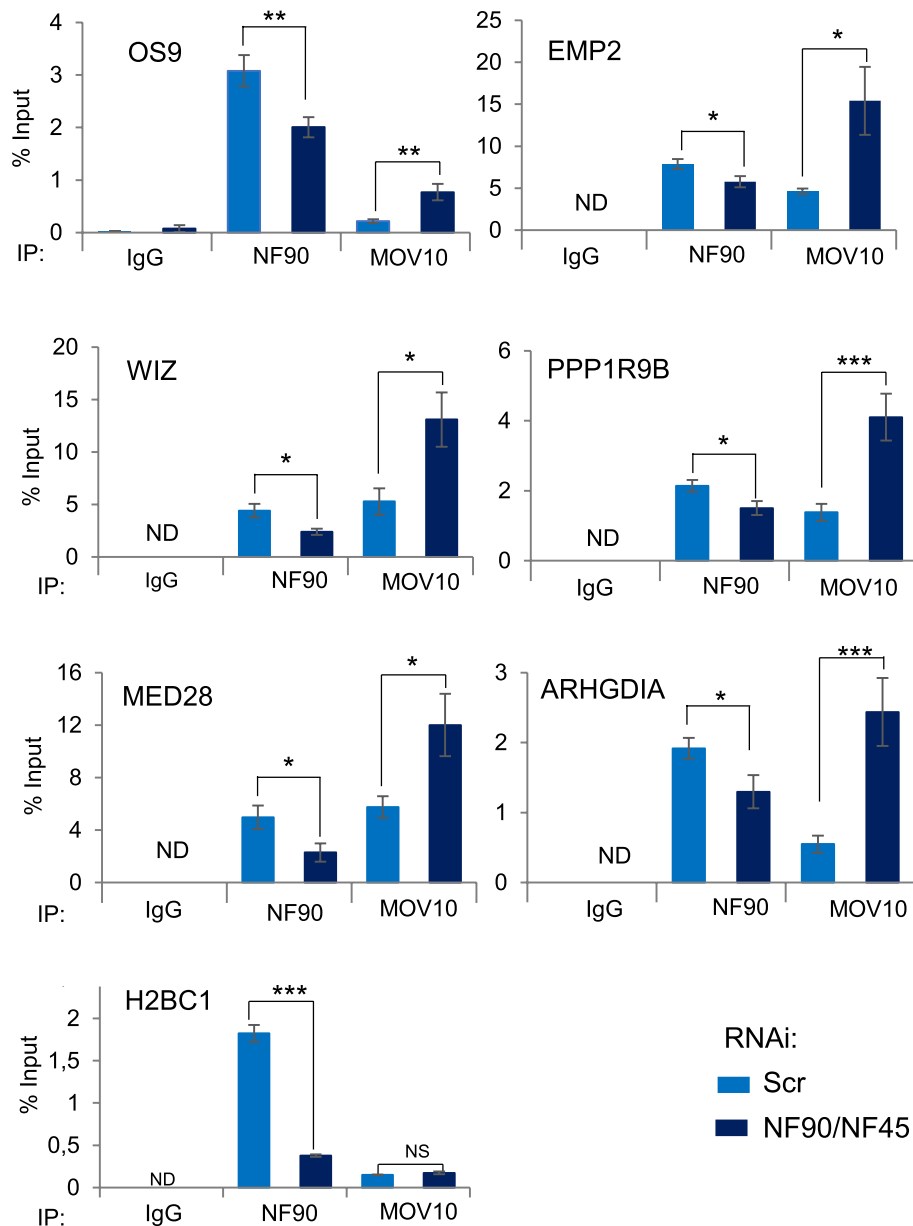


Fig. 4 NF90 modulates MOV10 association with common target mRNAs. RIP analysis of HEK293T cells transfected with NF90/NF45-targeting siRNAs or a non-targeting control (Scr), as indicated. RIPs were performed using anti-NF90, anti-MOV10 or a control IgG antibody. An aliquot of input and immunoprecipitates were analyzed using RT-qPCR using specific primers, as indicated. ND indicates "Not Detected." Data represent mean \pm SEM obtained from 4 independent experiments (* $P < 0.05$, ** $P < 0.01$, *** $P < 0.001$, NS indicates not significant, independent Student's t test) (Additional file 9).

performs these roles, we identified the interactome of cytoplasmic NF90. Identification of its partners may shed light on mechanisms by which NF90 is implicated in different pathways. Gene ontology analysis of the interactants revealed, not surprisingly, that almost all NF90 partners are involved in the processing, stability, or translation of cellular RNA, consistent with the known

functions of NF90. Interestingly, pathways associated with viral transcription and viral translation (Fig. 1A) were among the significantly enriched gene ontology terms. This is notable since it has been shown that NF90 translocates from the nucleus to the cytoplasm as a consequence of viral infection and, following its nuclear export, NF90 was shown to bind viral mRNAs, playing a

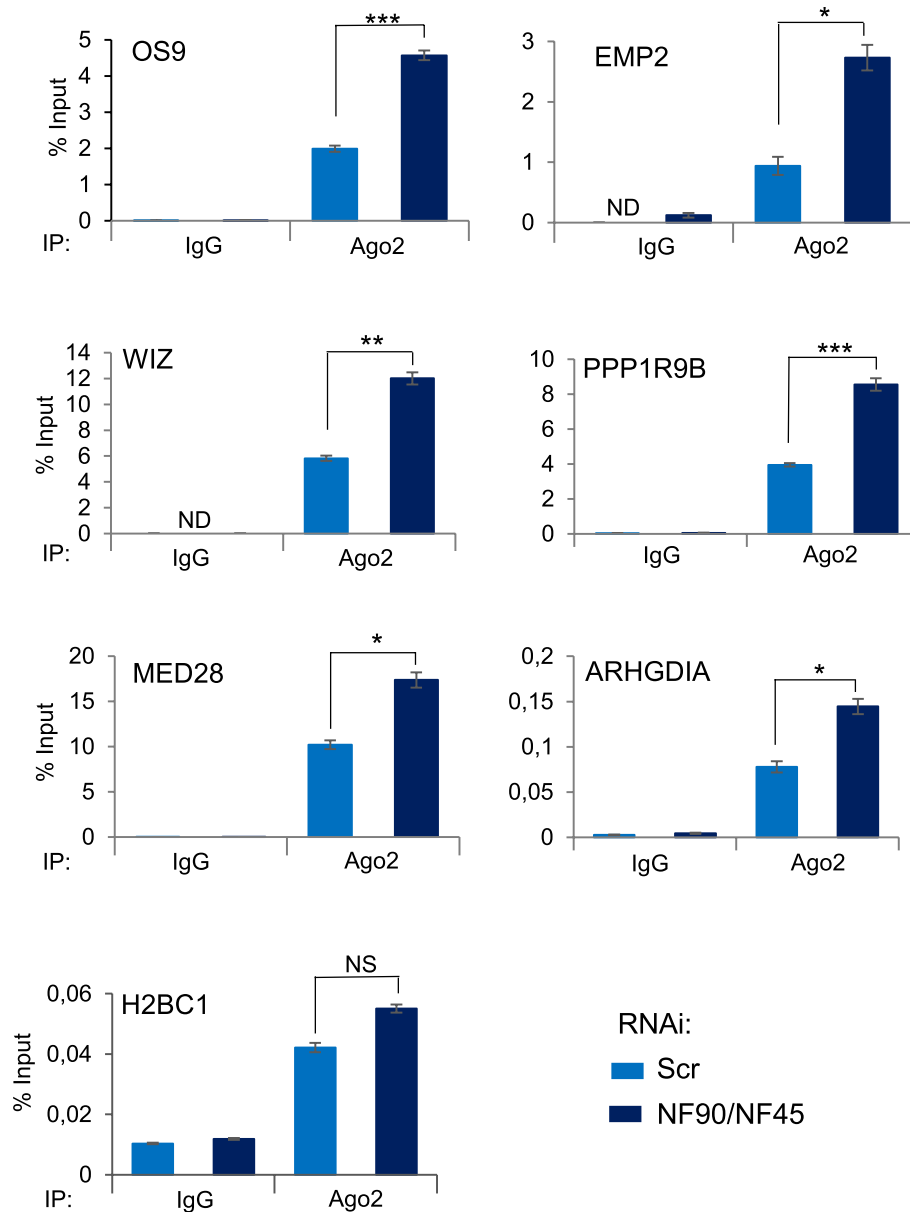


Fig. 5 Downregulation of NF90/NF45 increases Ago2 binding to selected target mRNAs. RIP analysis of HEK293T cells transfected with NF90/NF45-targeting siRNAs or a non-targeting control (Scr), as indicated. RIPs were performed using anti-Ago2 or a control IgG antibody. Immunoprecipitates were analyzed using RT-qPCR. ND indicates 'Not Detected'. Data represent mean \pm SEM obtained from 3 independent experiments (* $P < 0.05$, ** $P < 0.01$, *** $P < 0.001$, NS indicates not significant, independent Student's t test) (Additional file 9)

role in the antiviral immune response or enhancing viral replication, depending on the virus [2, 30]. We previously showed that nuclear NF90 is able to inhibit the biogenesis of several miRNAs involved in viral replication and antiviral response, such as miR-4753 and miR-3145 [13]. Consistently, these miRNAs were shown to be overexpressed in response to viral infection, inhibiting influenza A viral transcription and replication [31]. Thus, the identification of cytoplasmic NF90 partners involved in viral

transcription and translation suggests that NF90 may play an important role in the cellular response to viral infection.

NF90 has been implicated in the regulation of translation and mRNA stability. Moreover, a recent study put forward the hypothesis that this might be due to its involvement in miRNA-mediated gene silencing [16]. However, a direct role for NF90 in RISC-mediated silencing had not so far been demonstrated. The interactome

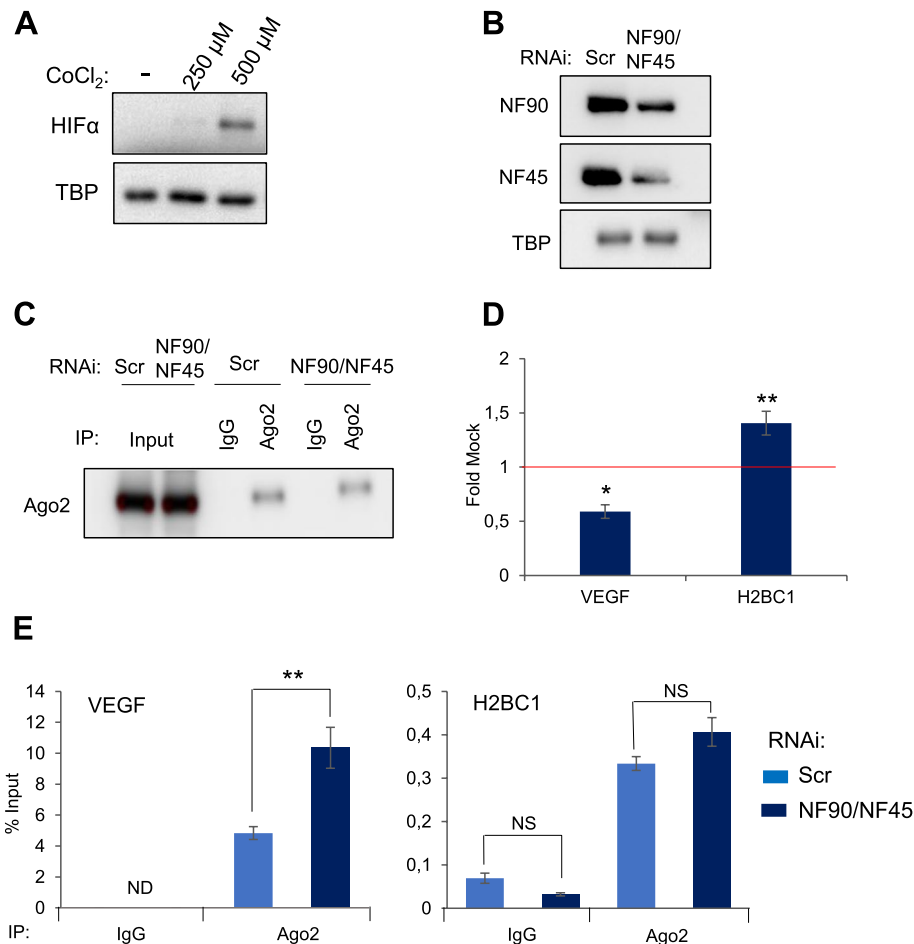


Fig. 6 NF90/NF45 impedes binding of Ago2 to VEGF mRNA during hypoxia. **A** Extracts of HEK293T cells treated with different concentrations of CoCl_2 , as indicated, were analyzed by Western blot using antibodies to HIF1 α and TBP. **B** Extracts of HEK293T cells transfected with siRNAs targeting NF90/NF45 or a non-targeting control (Scr) and treated with CoCl_2 were analyzed by Western blot using the indicated antibodies. **C** Immunoprecipitates obtained using anti-Ago2 or control IgG antibodies from extracts described in **(B)** were analyzed by Western blot using the indicated antibodies. **D** Total RNA obtained from HEK293T transfected with siRNAs targeting NF90 and NF45 or a non-targeting control (Scr) and treated with CoCl_2 were analyzed by RT-qPCR. Data represent fold mock (IgG) relative to the control samples (siScr), which was attributed a value of 1 (red line), obtained from 3 independent experiments ($*P < 0.05$, $***P < 0.01$, independent Student's *t* test) (Additional file 9). **E** RIP analysis of HEK293T cells transfected with NF90/NF45-targeting siRNAs or a non-targeting control (Scr), as indicated, and treated with CoCl_2 , RIPs were performed using anti-Ago2 or a control IgG antibody. Immunoprecipitates were analyzed using RT-qPCR. ND indicates 'Not Detected'. Data represent mean \pm SEM obtained from 3 independent experiments ($*P < 0.05$, $***P < 0.01$, $****P < 0.001$, NS indicates Not Significant, independent Student's *t* test) (Additional file 9)

of cytoplasmic NF90 contained several components of RISC. These include DHX30, UPF1, and DDX6 as well as the RISC-associated RNA helicase, MOV10. The effector of RISC-mediated silencing, Ago2, was also identified among NF90 interactants, which confirms previous reports identifying an interaction between NF90 and Ago2 [16, 23]. We furthermore determined that the association of NF90 with MOV10 and Ago2 occurs through RNA. NF90 likely exists in a cytosolic complex with RISC and RISC-associated proteins since these factors co-sediment in a glycerol gradient. These data suggest that NF90

may be linked to RISC-mediated silencing via RNA-dependent interactions with RISC-associated proteins.

Analysis of NF90 and MOV10 CLIP data suggested that both proteins can associate with the 3' UTR of a subset of target mRNAs. It should be noted, however, that the CLIP data were obtained in different cell types, HEK293T and HepG2, and although the comparative analysis shows that the target mRNAs selected for analysis are expressed in both cell types, the possibility remains that the 3' UTR may not be same in both cell types, due to alternative splicing or polyadenylation of

the pre-mRNA transcripts. Bearing this limitation in mind, our analysis suggests that NF90 increases mRNA stability while MOV10 enhances RISC-mediated silencing. Since these effects appear contradictory, we wondered whether NF90 and MOV10 could compete for the binding of selected target mRNAs. Upon downregulation of MOV10, an increase in the association of NF90 to the target mRNAs was detected. Likewise, upon loss of the heterodimer NF90/NF45, an increase in MOV10 binding to the same mRNAs was measured. These findings suggest that NF90 and MOV10 might influence or interfere with the ability of the other factor to associate with its target RNAs. This interference is unlikely to occur through direct competition for the same binding sites, as reported for NF90 and Microprocessor binding to pri-miRNAs in the nucleus [3, 13, 32]. Indeed, the binding preferences for NF90 and MOV10 differ significantly. MOV10 binds ssRNA upstream of a structured region while NF90 appears to bind highly stable hairpin structures [13, 14]. The binding of one factor may modify RNA structure to disfavor binding of the other. Alternatively, one factor may recruit additional proteins that may influence the binding of the other factor. For example, it has been shown that, although HuR and RISC have different binding sites, they compete for the binding of mRNA substrates [33]. Competition at distal sites could result from a conformational change of the RNA, following the binding of one factor, to disfavor the binding of the other factor. Additionally, binding of AUF1 has been shown to remodel the conformation of target mRNA substrates and affect the assembly of RNP complexes [34]. Therefore, although the precise mechanism is not clear, our data suggest that NF90 and MOV10 mutually interfere with each other's binding to a subset of common target mRNAs.

MOV10 helicase activity is known to resolve mRNA structures in order to reveal obscured MREs within 3' UTRs, which is thought to facilitate the binding of Ago2 and favor RISC-mediated silencing. Although loss of MOV10 could therefore be expected to enhance the stability of target mRNAs, we did not observe any significant increase in the abundance of the target mRNAs tested. However, the effect of MOV10 on mRNA stability is complex and may depend on several factors. While downregulation of MOV10 has been shown to increase target mRNA stability [23], others show that loss of MOV10 could lead to downregulation of the targeted mRNA, presumably by facilitating access of AGO2 [26, 35]. Interestingly, recent evidence suggests that binding of MOV10 to target mRNAs can either increase or decrease their RISC-mediated silencing, depending on the vicinity of the binding sites or the presence of additional proteins in the complex [25].

Depletion of NF90 significantly increased the association of MOV10, as well as Ago2, with target mRNAs. Consistent with increased Ago2 association, downregulation of the total level of the selected target mRNAs upon loss of NF90 was detected. These data suggest that NF90 enhances the stability of certain mRNAs by modulating the ability of Ago2 to associate with its target site and induce RISC-mediated silencing. However, although association of Ago2 with the target mRNAs was increased following loss of NF90, it remains to be determined whether the decrease in mRNA expression is a result of miRNA-mediated silencing. It is interesting to note that NF90 has been identified as a subunit of P-bodies [36]. P-bodies are a site of mRNA storage as well as RISC-mediated mRNA degradation. It is tempting to speculate that NF90 within P-bodies may be implicated in the control of mRNA stability versus degradation by modulating the binding of RISC. It would also be interesting to determine whether the destabilization of mRNAs observed upon loss of NF90 occurs within P-bodies.

Our data show that the binding of NF90 to target mRNA is associated with reduced binding of MOV10 and Ago2 to the same targets and, under the same conditions, the level of target mRNA changes accordingly. However, it should be noted that, the correlative nature of these data does not address whether the modulation of the target mRNA level is a direct effect of NF90 abundance or whether other mechanisms may also be involved. Furthermore, although increased binding of NF90 correlated with decreased binding of Ago2 and increased abundance of target mRNAs, our data do not conclusively show that this mechanism occurs through miRNA-mediated post-transcriptional repression.

NF90 is known to translocate to the cytoplasm during cancer-induced hypoxia where it can bind and stabilize VEGF [5, 6]. Interestingly, we found that during hypoxia, loss of NF90/NF45 diminished VEGF mRNA abundance, while its association with Ago2 was significantly increased. These results suggest that the role of NF90 in stabilizing VEGF during cancer-induced hypoxia might be the result of NF90 interfering with Ago2 binding to VEGF mRNA and, consequently, reduced targeting of VEGF mRNA by RISC activity. Therefore, better understanding of the role of NF90 in RISC-mediated silencing could potentially elucidate its effect on the fate of mRNAs involved in the antiviral immune response or during hypoxia induced in solid tumors.

Conclusions

NF90 is a dsRBP that has been described to be involved in a plethora of cellular pathways such as transcription, miRNA biogenesis, viral infection, and diseases. NF90 has already been shown to be implicated in the regulation

of mRNA stability and translation, recently involving miRNA activity. Here, we further elucidated the role of NF90 in mRNA stability. Cytoplasmic NF90 interacted with proteins involved in RISC activity, such as Ago2 and MOV10, in an RNA-dependent manner. In addition, CLIP analysis suggest that NF90 and MOV10 could potentially bind the same target mRNA. Interestingly, the binding of NF90 to target mRNA impaired the binding of MOV10 and Ago2 to the same targets and affected their abundance. These results suggest a role for NF90 in RISC-mediated silencing for a subset of target mRNAs.

Methods

Cell culture, stable cell line production and cellular treatments

Human HEK293T cell line was grown in Dulbecco's Modified Eagle's Medium containing high glucose with HEPES modification (Sigma-Aldrich[®], D6171), supplemented with 10% fetal bovine serum (PAN Biotech, 8500-P131704), 1% penicillin-streptomycin (v/v) (Sigma Aldrich[®], P4333), and 1% L-glutamine (v/v) (Sigma Aldrich[®], G7513). Cells were cultured at 37°C in a humidified atmosphere containing 5% CO₂. For experiments using RNAi, 3 × 10⁶ cells were seeded in 100 mm culture dishes at the day of siRNA transfection or at 5 × 10⁶ cells for experiments using RNAi together with CoCl₂ treatment.

Plasmid encoding pOZ-NF90-FLAG-HA (pOZ-NF90-FH) was cloned using pOZ-N-FH vector, as previously described [37]. Briefly, lentiviral particles expressing NF90 were produced in HEK293T cells by transfecting plasmids using calcium-phosphate. HEK293T were transduced using Polybrene infection/transfection reagent (Sigma-Aldrich[®], TR-1003), according to the manufacturer's instructions. After 7 days, selection of transduced cells was carried out by magnetic affinity sorting with antibody against IL2 to achieve a pure population. HEK293T stably expressing NF90 (pOZ-NF90-Flag-HA HEK293T) were grown in the same conditions as HEK293T. pOZ-NF90-FH HEK293T were seeded at 1 × 10⁷ in 150 mm culture dishes the day prior to protein extraction. For hypoxia treatment, HEK293T were treated for 24 h with 500 μM of CoCl₂ (Sigma, 15862-1ML-F) or the same volume of water as a control, where indicated.

Transfection of small interfering RNAs

Double-stranded RNA oligonucleotides used for RNAi were purchased from Eurofins MWG Operon or Integrated DNA Technologies. Sequences of siRNAs used in this study have been described previously [13] and are shown in Additional file 8: Table S1. HEK293T cells were transfected with siRNA (30 nM final concentration) using

INTERFERin[®] siRNA transfection reagent (PolyPlus Transfection) according to the manufacturer's instructions. The transfection was carried out the day of seeding and cells were collected for protein extraction approximately 65 h after transfection.

Immunoblot

HEK293T and pOZ-NF90-FH HEK293T were lysed using RIPA buffer (50 mM Tris-HCl pH = 7.5, 150 mM NaCl, 1 % NP40, 0.5 % Sodium Deoxycholate, 0.1 % SDS, Halt[™] Phosphatase Inhibitor Cocktail (Thermo Fisher Scientific)), unless otherwise indicated. Protein extracts were immunoblotted using the indicated primary antibodies (Additional file 8: Table S2) and anti-mouse, anti-rabbit or anti-rat IgG-linked HRP secondary antibodies (GE Healthcare) followed by ECL (Advansta).

Cytoplasmic extracts and co-immunoprecipitation analysis

HEK293T were seeded in 150 mm culture dishes the day prior to protein extraction. Cytoplasmic proteins were extracted using a mild lysis buffer (10 mM Hepes pH 7.9, 10 mM KCl, 0.1 mM EDTA pH 8.0, 2 mM MgCl₂, 1 mM DTT, EDTA-free protease and phosphatase inhibitor). The cell pellet was incubated for 10 min on ice, adding 0.07% NP-40 and incubating for additional 10 min on ice. After centrifugation, 1 mg of lysates were incubated at 4°C overnight with 2 μg of antibodies recognizing NF90, Ago2, and IgG controls and protein A/G PLUS-Agarose beads (Santa Cruz, sc-2003). Beads were then washed twice with IP buffer (150 mM KCl, 20 mM Tris pH 7.5, 0.05% NP-40, 0.1% Tween, 10% glycerol, 5 mM MgCl₂, 1 mM DTT, and EDTA-free protease and phosphatase inhibitor). Samples were treated with RNase A/T1 mix (ThermoFisher Scientific, EN0551) for 30 min at room temperature, incubating on a rotating wheel. After incubation, beads were washed three times with IP buffer as aforementioned and 2X Laemmli buffer was added directly to the beads.

Tandem Immunoprecipitation and mass spectrometry

For mass spectrometry, cytoplasmic extracts were obtained as aforementioned. Tandem immunoprecipitation (Flag and HA) was carried out using 10 mg of cytoplasmic extract. Flag IP was performed using EZview[™] Red ANTI-Flag[®] M2 Affinity gel (SigmaAldrich, F2426), following the manufacturer's instructions. Washes were carried out 3 times as aforementioned and protein complexes were eluted by competition performing 2 consecutive elutions using Flag elution buffer (250 ng/μl FLAG[®] Peptide (SigmaAldrich, F3290), diluted in IP buffer) incubating for 1 h at 4°C on a rotating wheel. HA IP was performed using the elutions obtained from the first IP incubated with Pierce[™] Anti-HA Agarose beads

(ThermoScientific, 26181) for 2 h at 4°C on a rotating wheel. Washes were carried out 5 times as aforementioned and elutions were performed using HA elution buffer (400 ng/μl HA peptide (ThermoScientific, 26184), diluted in IP buffer) for 1 h at 4°C on a rotating wheel. Following elution, beads were removed using Pierce™ Centrifuge Columns (ThermoScientific, 11894131), as specified by manufacturer's instructions. Silver-staining was performed according to the manufacturer's instructions (Silverquest, Invitrogen). Mass spectrometry was performed at Taplin facility, Harvard University, Boston, MA.

Glycerol gradient sedimentation

Glycerol gradient sedimentation was performed as described previously [37]. Briefly, NF90-associated proteins were purified by performing FLAG IP on pOZ-NF90-FH HEK293T cytoplasmic fraction, as aforementioned. One ml layers of glycerol (final concentration 15 to 35%–20 mM Tris pH 7.5, 0.15 M KCl, 2.5 mM MgCl₂, 0.05% NP-40, 0.1% Tween) were layered into centrifugation tubes (13 × 51 mm Ultra-Clear Tubes, Beckman). A linear gradient was obtained after 12 h of diffusion at 4°C. Flag elution from pOZ-NF90-FH HEK293T immunoprecipitation was loaded on top of the glycerol gradient. Complexes were fractionated by ultracentrifugation in an SW 55Ti rotor (Beckman) at 30,000 rpm for 18 h at 4°C. 25 fractions of 200 μL were collected from top of the gradient. An equal volume of fractions was resolved by SDS-PAGE and immunoblotted with indicated antibodies.

RNA immunoprecipitation

RIP was performed as previously described [13]. Briefly, HEK293T were seeded in 100 mm culture dishes and transfected with siRNAs the day of seeding or treated with CoCl₂, as aforementioned. Cells were harvested ~65 h after the siRNA treatment or 24 h after CoCl₂ treatment and lysed for 10 min in RIP buffer (20 mM HEPES, pH 7.5, 150 mM NaCl, 2.5 mM MgCl₂•6H₂O, 250 mM sucrose, 0.05% (v/v) NP-40 and 0.5% (v/v) Triton X-100) containing 20 U ml⁻¹ of RNasin (Promega), 1 mM DTT, 0.1 mM PMSF and EDTA-free protease and phosphatase inhibitor. After centrifugation, lysates were incubated overnight at 4°C with 2 μg of antibodies recognizing NF90, MOV10, Ago2, and IgG control and then incubated for 1 h at 4°C with Dynabeads™ Protein A or G (ThermoFisher Scientific). After incubation, beads were washed five times with RIP buffer for 5 min at 4°C, and RNA was extracted using TRIzol (Thermo Fisher Scientific) according to the manufacturer's instructions. RNA was treated with DNase I (Promega) and RT was performed using SuperScript™ III Reverse Transcriptase

(ThermoFisher Scientific) according to the manufacturer's instructions. cDNA was treated with RNase H (ThermoFisher Scientific) and the samples were used to perform qPCR using LightCycler™ 480 SYBR Green I Master mix (Roche), according to the manufacturer's instructions, using the primers shown in Additional file 8: Table S3.

Bioinformatic analyses

Enhanced UV crosslinking followed by immunoprecipitation (eCLIP) data for NF90 were obtained from Nussbacher and Yeo [29] and retrieved from the NCBI database (NF90 eCLIP: ENCSR786TSC). Individual-nucleotide-resolution UV crosslinking (iCLIP) data for MOV10 were obtained and retrieved from the NCBI database (MOV10 iCLIP: GSE51443). MOV10 iCLIP data was lifted to hg38 genome annotation using UCSC liftOver tool. Peaks were filtered based on Fold Change (FC ≥ 1.5) and *p*-value (Bonferroni-Adj *P*-val ≤ 0.05). Bigwig files from different replicates were merged using bigWigMerge v2. Statistical analyses were performed using RStudio v1.4. Gene ontology was performed using DAVID Functional Annotation Tool database version 6.8 (<https://david.ncifcrf.gov>).

Abbreviations

AGO2: Argonaute 2; ARHGDI: Rho GDP dissociation inhibitor alpha; circRNA: Circular RNA; DDX6: DEAD-box helicase 6; DHX30: DexH-box helicase 30; dsRBM: Double-stranded RNA-binding motif; eCLIP: Enhanced UV crosslinking and IP; EMP2: Epithelial membrane protein 2; FMRP1: Fragile X mental retardation protein 1; H2BC1: H2B clustered histone 1; iCLIP: Individual-nucleotide resolution UV crosslinking and IP; MED28: Mediator complex subunit 18; miRNA: MicroRNA; MOV10: Moloney leukemia virus 10; MRE: miRNA recognition element; NF45: Nuclear factor 45; NF90: Nuclear factor NF90; OS9: Osteosarcoma amplified 9; PPP1R9B: Protein phosphatase 1 regulatory subunit 9B; qPCR: Quantitative PCR; RBP: RNA-binding protein; RIP: RNA immunoprecipitation; RISC: RNA-induced silencing complex; siRNA: Small interfering RNA; SMD: Staufen-mediated mRNA decay; ssRNA: Single-strand RNA; UPF1: UP-frameshift-1; UTR: Untranslated region; VEGF: Vascular endothelial growth factor; WIZ: WIZ zinc finger.

Supplementary Information

The online version contains supplementary material available at <https://doi.org/10.1186/s12915-022-01384-2>.

Additional file 1: Fig. S1. NF90 interacts with proteins involved in translational repression and RNA processing. (A) Cytoplasmic and nuclear extracts of WT (mock) and NF90-FH stably overexpressing (NF90-FH) HEK293T cells were analyzed by Western blot using the indicated antibodies. (B) Cytoplasmic extracts described in A underwent tandem affinity purification using FLAG and HA antibodies. Samples were analyzed by western blot using the indicated antibodies (FT = flow through, E1 = elution 1; E2 = elution 2). (C) Molecular functions of NF90-associated proteins (*n* = 209; 3 or more peptides, FC > 2) identified by mass spectrometry were analyzed using gene ontology. (D) Cytoplasmic extracts of NF90-FH overexpressing HEK293T cells used for FLAG immunoprecipitation followed by glycerol gradient sedimentations were analyzed by western blot using the antibodies indicated. (E) An aliquot of FLAG immunoprecipitate from NF90-FH overexpressing HEK293T cells used for glycerol gradient

sedimentation were analyzed by western blot, using the antibodies indicated (In = input, FT = flowthrough, E = elution).

Additional file 2: Fig. S2. NF90 and MOV10 can bind the same target mRNAs. Screenshots of NF90 and MOV10 eCLIP and iCLIP, respectively, showing regions associated with NF90 (green bars) and MOV10 (red bars) within selected target mRNAs. Introns are shown as thin lines, 5' and 3' UTRs are shown as medium lines and exons are shown as thick lines. The orientation of the transcript with respect to the genome is indicated by arrows.

Additional file 3: Fig. S3. MOV10 modulates NF90 association with common target mRNAs. (A) Extracts of HEK293T cells transfected with siRNAs targeting MOV10 or a nontargeting control (Scr) and immunoprecipitates obtained using antibodies anti-NF90, anti-MOV10 or control IgG were analyzed by Western blot using the indicated antibodies. (B) Total RNA obtained from HEK293T transfected with siRNAs targeting MOV10 or a non-targeting control (Scr) was analyzed by RT-qPCR using transcript specific PCR primers, as indicated. Values obtained in MOV10 knock-down condition were calculated relative to the control samples (siScr), which was attributed a value of 1 (red line). Data represent the mean \pm SEM obtained from 4 independent experiments (NS indicates 'Not Significant', independent Student's *t* test) (Additional file 9).

Additional file 4: Fig. S4. MOV10 modulates NF90 association with common target mRNAs. (A) Extracts of HEK293T cells transfected with siRNAs targeting MOV10 (MOV10#2) or a non-targeting control (Scr) and immunoprecipitates obtained using antibodies against NF90, MOV10 or control IgG were analyzed by Western blot using the indicated antibodies. (B) RIP analysis of HEK293T cells transfected with MOV10-targeting siRNA (MOV10 #2) or a non-targeting control (Scr), as indicated. RIPs were performed using anti-NF90, anti-MOV10 or a control IgG antibody, as indicated. An aliquot of input and Immunoprecipitates were analyzed using RT-qPCR using transcript-specific primers. Data represent mean \pm SEM obtained from $n > 6$ independent experiments (* $P < 0.05$, ** $P < 0.01$, *** $P < 0.001$, NS indicates Not Significant, independent Student's *t* test).

Additional file 5: Fig. S5. NF90 modulates MOV10 association with common target mRNAs. (A) Extracts of HEK293T cells transfected with siRNAs targeting NF90 and NF45 (siNF90#2/NF45#2) or a non-targeting control (Scr) and immunoprecipitates obtained using antibodies anti-NF90, anti-MOV10 or control IgG were analyzed by Western blot using the indicated antibodies. (B) Total RNA obtained from HEK293T transfected with siRNAs targeting NF90 and NF45 or a non-targeting control (Scr) was analyzed by RT-qPCR using transcript-specific PCR primers, as indicated. Values obtained in NF90/NF45 knock-down condition were calculated relative to the control samples (siScr), which was attributed a value of 1 (red line). Data represent the mean \pm SEM obtained from 4 independent experiments (* $P < 0.05$, ** $P < 0.01$, *** $P < 0.001$, NS indicates Not Significant, independent Student's *t* test) (Additional file 9).

Additional file 6: Fig. S6. NF90 modulates MOV10 association with common target mRNAs. (A) Extracts of HEK293T cells transfected with siRNAs targeting NF90 and NF45 (siNF90#2/NF45#2) or a non-targeting control (Scr) and immunoprecipitates obtained using anti-NF90, anti-MOV10 or control IgG were analyzed by Western blot using the indicated antibodies. (B) RIP analysis of HEK293T cells transfected with NF90/NF45-targeting siRNAs (siNF90#2/NF45#2) or a non-targeting control (Scr), as indicated. RIPs were performed using anti-NF90, anti-MOV10 or a control IgG antibody. An aliquot of input and Immunoprecipitates were analyzed using RT-qPCR. ND indicates 'Not Detected'. Data represent mean \pm SEM obtained from $n > 6$ independent experiments (* $P < 0.05$, ** $P < 0.01$, *** $P < 0.001$, NS indicates Not Significant, independent Student's *t* test).

Additional file 7: Fig. S7. Downregulation of NF90/NF45 does not affect the expression of Ago2 (A) Extracts of HEK293T cells transfected with siRNAs targeting NF90/NF45 or a nontargeting control (Scr) were analyzed by Western blot using the indicated antibodies. (B) Immunoprecipitates obtained using anti-Ago2 or control IgG antibodies from extracts of HEK293T cells transfected with siRNAs targeting NF90/NF45 or a non-targeting control (Scr) were analyzed by Western blot using anti-Ago2 antibody.

Additional file 8: Table S1. Double stranded siRNAs used in this study.

Table S2. Primary antibodies used in this study. **Table S3.** Primers used in this study. **Table S4.** Proteins associated with NF90 in the cytoplasm, detected by tandem affinity purification followed by tandem mass spectrometry. Number of peptides refers to the number of unique peptides identified in the NF90 sample. Fold change indicates the number of peptides detected in the NF90 sample divided by the number of peptides detected in the mock control sample. ND in control indicates that no peptides were detected in the control sample.

Additional file 9.

Acknowledgements

The authors thank Claudio Lorenzi for bioinformatic assistance Thomas Lecesne for technical assistance and members of the Gene Regulation lab for helpful discussions.

Authors' contributions

GG and CA performed the experiments and contributed to writing the manuscript; CF helped with glycerol gradient sedimentation and RIP experiments; RNS helped with creating the stable cell line overexpressing NF90-FH and mass spectrometry; MB helped with the RIP experiments; JB created the stable cell line overexpressing NF90-FH and prepared samples for mass spectrometry; RK designed the study and wrote the manuscript. All authors read and approved the final manuscript.

Funding

This study was supported by funds from MSDAvenir and the European Research Council (RNAmEdTGS) to R.K., Ministère de l'Enseignement Supérieur et de la Recherche et de l'Innovation (MESRI) scholarship and Association pour la Recherche contre le Cancer (ARC) to G.G., and ANRS fellowship to C.A.

Availability of data and materials

All data generated or analyzed during this study are included in this published article, its supplementary information files and publicly available repositories. Supporting data values: Additional file 9
MOV10 iCLIP: GSE51443 [26]
NF90 eCLIP: ENCSR786TSC [29]

Declarations

Ethics approval and consent to participate

Not applicable.

Consent for publication

Not applicable.

Competing interests

The authors declare that they have no competing interests.

Received: 22 September 2021 Accepted: 5 August 2022

Published online: 01 September 2022

References

- Castella S, Bernard R, Corno M, Fradin A, Larcher JC. Iif3 and NF90 functions in RNA biology. *Wiley Interdiscip Rev RNA*. 2015;6:243–56. <https://doi.org/10.1002/wrna.1270>.
- Li X, Liu CX, Xue W, Zhang Y, Jiang S, Yin QF, et al. Coordinated circRNA biogenesis and function with NF90/NF110 in viral infection. *Mol Cell*. 2017;67(2):214–227.e217.
- Sakamoto S, Aoki K, Higuchi T, Todaka H, Morisawa K, Tamaki N, et al. The NF90-NF45 complex functions as a negative regulator in the microRNA processing pathway. *Mol Cell Biol*. 2009;29(13):3754–69.
- Harashima A, Guettouche T, Barber GN. Phosphorylation of the NFAR proteins by the dsRNA-dependent protein kinase PKR constitutes a novel mechanism of translational regulation and cellular defense. *Genes Dev*. 2010;24(23):2640–53.

5. Vrakas CN, Herman AB, Ray M, Kelemen SE, Scalia R, Autieri MV. RNA stability protein ILF3 mediates cytokine-induced angiogenesis. *FASEB J*. 2019;33(3):3304–16.
6. Zhang W, Xiong Z, Wei T, Li Q, Tan Y, Ling L, et al. Nuclear factor 90 promotes angiogenesis by regulating HIF-1 α /VEGF-A expression through the PI3K/Akt signaling pathway in human cervical cancer. *Cell Death Dis*. 2018;9(3):276.
7. Patino C, Haenni AL, Urcuqui-Inchima S. NF90 isoforms, a new family of cellular proteins involved in viral replication? *Biochimie*. 2015;108:20–4.
8. Song D, Huang H, Wang J, Zhao Y, Hu X, He F, et al. NF90 regulates PARP1 mRNA stability in hepatocellular carcinoma. *Biochem Biophys Res Commun*. 2017;488(1):211–7.
9. Vumbaca F, Phoenix KN, Rodriguez-Pinto D, Han DK, Claffey KP. Double-stranded RNA-binding protein regulates vascular endothelial growth factor mRNA stability, translation, and breast cancer angiogenesis. *Mol Cell Biol*. 2008;28(2):772–83.
10. Nourredine S, Lavoie G, Paradis J, Ben El Kadhi K, Meant A, Aubert L, et al. NF45 and NF90 regulate mitotic gene expression by competing with Staufen-mediated mRNA decay. *Cell Rep*. 2020;31(7):107660.
11. Jayachandran U, Grey H, Cook AG. Nuclear factor 90 uses an ADAR2-like binding mode to recognize specific bases in dsRNA. *Nucleic Acids Res*. 2016;44(4):1924–36.
12. Schmidt T, Knick P, Lilie H, Friedrich S, Golbik RP, Behrens SE. Coordinated action of two double-stranded RNA binding motifs and an RGG motif enables nuclear factor 90 to flexibly target different RNA substrates. *Biochemistry*. 2016;55(6):948–59.
13. Grasso G, Higuchi T, Mac V, Barbier J, Helmsmoortel M, Lorenzi C, et al. NF90 modulates processing of a subset of human pri-miRNAs. *Nucleic Acids Res*. 2020;48(12):6874–88.
14. Gwizdek C, Ossareh-Nazari B, Brownawell AM, Evers S, Macara IG, Dargemont C. Minihelix-containing RNAs mediate exportin-5-dependent nuclear export of the double-stranded RNA-binding protein ILF3. *J Biol Chem*. 2004;279(2):884–91.
15. Schmidt T, Knick P, Lilie H, Friedrich S, Golbik RP, Behrens SE. The properties of the RNA-binding protein NF90 are considerably modulated by complex formation with NF45. *Biochem J*. 2017;474(2):259–80.
16. Idda ML, Lodde V, McClusky WG, Martindale JL, Yang X, Munk R, et al. Cooperative translational control of polymorphic BAFF by NF90 and miR-15a. *Nucleic Acids Res*. 2018;46(22):12040–51.
17. Flores O, Kennedy EM, Skalsky RL, Cullen BR. Differential RISC association of endogenous human microRNAs predicts their inhibitory potential. *Nucleic Acids Res*. 2014;42(7):4629–239.
18. Bartel DP. MicroRNAs: target recognition and regulatory functions. *Cell*. 2009;136(2):215–33.
19. Hock J, Weinmann L, Ender C, Rudel S, Kremmer E, Raabe M, et al. Proteomic and functional analysis of Argonaute-containing mRNA-protein complexes in human cells. *EMBO Rep*. 2007;8(11):1052–60.
20. Gregersen LH, Schueler M, Munschauer M, Mastrobuoni G, Chen W, Kempa S, et al. MOV10 is a 5' to 3' RNA helicase contributing to UPF1 mRNA target degradation by translocation along 3' UTRs. *Mol Cell*. 2014;54(4):573–85.
21. Huang F, Zhang J, Zhang Y, Geng G, Liang J, Li Y, et al. RNA helicase MOV10 functions as a co-factor of HIV-1 Rev to facilitate Rev/RRE-dependent nuclear export of viral mRNAs. *Virology*. 2015;486:15–26.
22. Liu T, Sun Q, Liu Y, Cen S, Zhang Q. The MOV10 helicase restricts hepatitis B virus replication by inhibiting viral reverse transcription. *J Biol Chem*. 2019;294(51):19804–13.
23. Meister G, Landthaler M, Peters L, Chen PY, Urlaub H, Luhrmann R, et al. Identification of novel argonaute-associated proteins. *Curr Biol*. 2005;15(23):2149–55.
24. Yang Q, Jankowsky E. The DEAD-box protein Ded1 unwinds RNA duplexes by a mode distinct from translocating helicases. *Nat Struct Mol Biol*. 2006;13(11):981–6.
25. Kenny PJ, Kim M, Skariah G, Nielsen J, Lannom MC, Ceman S. The FMRP-MOV10 complex: a translational regulatory switch modulated by G-Quadruplexes. *Nucleic Acids Res*. 2020;48(2):862–78.
26. Kenny PJ, Zhou H, Kim M, Skariah G, Khetani RS, Drnevich J, et al. MOV10 and FMRP regulate AGO2 association with microRNA recognition elements. *Cell Rep*. 2014;9(5):1729–41.
27. Guan D, Altan-Bonnet N, Parrott AM, Arrigo CJ, Li Q, Khaleduzzaman M, et al. Nuclear factor 45 (NF45) is a regulatory subunit of complexes with NF90/110 involved in mitotic control. *Mol Cell Biol*. 2008;28(14):4629–41.
28. Wolkowicz UM, Cook AG. NF45 dimerizes with NF90, Zfr and SPNR via a conserved domain that has a nucleotidyltransferase fold. *Nucleic Acids Res*. 2012;40(18):9356–68.
29. Nussbacher JK, Yeo GW. Systematic discovery of RNA binding proteins that regulate MicroRNA levels. *Mol Cell*. 2018;69(6):1005–1016.e1007.
30. Isken O, Baroth M, Grassmann CW, Weinlich S, Ostareck DH, Ostareck-Lederer A, et al. Nuclear factors are involved in hepatitis C virus RNA replication. *RNA*. 2007;13(10):1675–92.
31. Khongnomnan K, Makkoch J, Poomipak W, Poovorawan Y, Payungporn S. Human miR-3145 inhibits influenza A viruses replication by targeting and silencing viral PB1 gene. *Exp Biol Med (Maywood)*. 2015;240(12):1630–9.
32. Barbier J, Chen X, Sanchez G, Cai M, Helmsmoortel M, Higuchi T, et al. An NF90/NF110-mediated feedback amplification loop regulates dicer expression and controls ovarian carcinoma progression. *Cell Res*. 2018;28(5):556–71.
33. Srikantan S, Tominaga K, Gorospe M. Functional interplay between RNA-regulate protein HuR and microRNAs. *Curr Protein Pept Sci*. 2012;13(4):372–9.
34. Zucconi BE, Ballin JD, Brewer BY, Ross CR, Huang J, Joth EA, et al. Alternatively expressed domains of AU-rich element RNA-binding protein 1 (AUF1) regulate RNA-binding affinity, RNA-induced protein oligomerization, and the local conformation of bound RNA ligands. *J Biol Chem*. 2010;285(50):39127–39.
35. Lannom MC, Nielsen J, Nawaz A, Shilkbay T, Ceman S. FMRP and MOV10 regulate Dicer1 expression and dendrite development. *PLoS One*. 2021;16(11):e0260005.
36. Hubstenberger A, Courel M, Benard M, Souquere S, Ernault-Lange M, Chouaib R, et al. P-Body purification reveals the condensation of repressed mRNA regulons. *Mol Cell*. 2017;68(1):144–157.e145.
37. Contreras X, Salifou K, Sanchez G, Helmsmoortel M, Beyne E, Bluy L, et al. Nuclear RNA surveillance complexes silence HIV-1 transcription. *PLoS Pathog*. 2018;14(3):e1006950.

Publisher's Note

Springer Nature remains neutral with regard to jurisdictional claims in published maps and institutional affiliations.

Ready to submit your research? Choose BMC and benefit from:

- fast, convenient online submission
- thorough peer review by experienced researchers in your field
- rapid publication on acceptance
- support for research data, including large and complex data types
- gold Open Access which fosters wider collaboration and increased citations
- maximum visibility for your research: over 100M website views per year

At BMC, research is always in progress.

Learn more biomedcentral.com/submissions

